

A Comparison of Interpolation Techniques in Producing a DEM from the 5 m National Geospatial Institute (NGI) Contours

Prevlan Chetty and Solomon Tesfamichael

Department of Geography, Environmental Management and Energy Studies,
University of Johannesburg, Johannesburg, South Africa

Keywords: GIS, Remote Sensing, Interpolation, LiDAR, Kriging, Inverse Distance Weighting, Spline, Nearest Neighbour, Topo to Raster, ANUDEM, Chief Directorate National Geospatial Information, NGI.

Abstract: Continuous elevation surfaces, which are commonly referred to as Digital Elevation Models (DEM), are vital sources of information in flood modelling. Due to the multitude of interpolation techniques available to create DEMs, there is a need to identify the best suited interpolation techniques to represent a localised hydrological environment. This study investigated the accuracies of commonly applied interpolation techniques including Inverse Distance Weighting (IDW), Nearest Neighbour (NN), Kriging, Spline and Topo to Raster interpolation techniques as applied to a 5-m interval elevation contours as a precursor to simulate a flood zone in the Roodepoort region in Johannesburg, South Africa. A 50 cm resolution DEM derived from aerial Light Detection and Ranging (LiDAR) point cloud was used as a reference to compare the five interpolations techniques. The Topo to Raster results were not significantly different from the reference data ($P = 0.79$ at 95% confidence level), where elevation values were on average underestimated by 0.93 m. In contrast, the spline interpolation showed the highest significant difference from the reference data ($P = 0.00$ at 95% confidence level), with an average underestimation of the elevation by 69.84 m. Outlier identification using standardized residual analysis flagged significant elevation outliers that were produced in the interpolation process, and it was noted that most of the outliers across all techniques coincide with areas that showed frequent topographical changes. Specifically, the largest significant differences using the Topo to Raster technique were overestimations of the elevation that occur in the upstream section of the tributary. The Spline technique in contrast showed significant underestimations of the elevation throughout the river system. Overall, the results indicate that the Topo to Raster technique is preferred to accurately represent the topography around a river system of the study area.

1 INTRODUCTION

Flooding is a globally occurring phenomenon that causes property loss and casualties all around the world (Teng *et al.*, 2017). A flood is characterised by an overflow of water that submerges land that would usually be dry which is often referred to as the flood inundation area (Merz and Blöschl, 2008). The extent to which a given river will flood to is commonly referred to as a flood-line (the maximum extent of the flood inundation area) and is related to the effect that a specific volume of water has on a hydrological system through rainfall events (Nkwunonwo *et al.*, 2020). The statistical likelihood of a rainfall volume is commonly translated to 10-Year, 50-Year and a 100-Year, and a flood event (Smithers, 2012). As part of South Africa's Council for Scientific and Industrial

Research's (CSIR) Guidelines for Human Settlement, Planning and Design (CSIR, 1999), no urban development should be allowed in the demarcated 50-year flood-line extent. The requirement itself originates from the National Building Regulation and Building Standards Act of South Africa (Act 103 of 1997) and is solely based on safety considerations. The establishment of the flood-line extents therefore play a crucial role in any development along a river.

In deterministic computer aided techniques of demarcating a flood-line, one of the most important aspects is the input elevation data that defines the geometry of the river and its surrounding basin (Saksena & Merwade, 2015). Flood-line mapping often produces results that vary with different sources of elevation data. The outputs are affected by the vertical accuracy which is determined by the

topography of the region and the spatial resolution of the elevation data (Li *et al.*, 2010). In addition, the importance of interpolation algorithm accuracy is recognised as an integral component in representing the topography in numerical form (Chaplot *et al.*, 2006). If interpolation forms an integral component of defining topography, and the topography forms an important part of the flood-line process, it can be inferred that the interpolation procedure of elevation data plays an important role in the development of flood-line extents.

For elevation data to be accurately incorporated into the flood-line modelling process, there needs to be spatial continuity in the elevation dataset by creating a raster surface referred to as a Digital Elevation Model (DEM). DEMs are derived through the process of interpolation, which refers to the prediction of a series of unknown values located between a limited number of sample points (Manuel, 2004). Interpolation techniques, of which numerous techniques are available, are commonly used for geographic data that are represented as points or lines having elevation information. These techniques are commonly grouped into local/global, deterministic/geostatistical and exact/approximate classes (Erdogan, 2009). Local methods of interpolation include the Inverse Distance Weighting (IDW) and the Nearest Neighbour (NN) technique. Geostatistical methods of interpolation include the kriging method, which uses the spatial location of data points rather than relying on the elevation attribute values alone (Arun, 2013). The spline (sometimes referred to as rubber sheet) method is mathematical in nature and takes the form of a cubic equation whereby each known data point has a cubic equation where all splines pass through (Robinson & Metternicht, 2003).

Different interpolation techniques applied to the same set of elevation data can result in varying DEM outputs (Arun, 2013). There is therefore a need to evaluate the suitability and accuracy of these interpolation techniques for a specific data and purpose. Erdogan (2009) investigated the relative accuracy of various interpolation algorithms for an area with high topographical variance in Turkey. The research evaluated various deterministic interpolation algorithms against a baseline survey grade dataset. The best results were obtained using the thin plate spline algorithm, a derivative of the spline algorithm itself. Zimmerman *et al.* (1999) compared the outputs of the IDW versus the kriging methodology and showed that the kriging method was able to adjust itself to the spatial variability of the data and by doing so, yielded better estimation of altitude for unknown

sample points. In contrast, Aguilar *et al.* (2005) presented research from their study area in Almeria, Spain, that indicated that the IDW method was marginally better than the accuracy from the kriging model output.

In 1984, Mark was the first to propose an algorithm for automatically delineating a drainage network from DEM data for specific applications in hydrological modelling (Mark, 1984). This study gave rise to the need for hydrological correction algorithms in the DEM interpolation process which includes the development of the Australian National University Digital DEM (ANUDEM), known as the Topo to Raster feature in ArcGIS, to generate elevation models that are hydrologically conducive to network extraction (Callow *et al.*, 2007). The ANUDEM method creates an interpolated surface that preserves the critical geometry components required to define a hydrological system which includes ridgelines and stream networks (Arun, 2013). Pavlova (2017) presented research conducted in the Omsk region in Russia which evaluated the outputs from IDW, Kriging, Topo To Raster, Spline, Nearest Neighbour (NN) and the Triangulated Irregular Network (TIN) techniques. The findings indicated that on relatively flat areas, the best results were obtained using the Spline and IDW techniques. In a contrasting environment, Salekin *et al.* (2018) conducted research into utilising Global Navigation Satellite Systems (GNSS) as a data source to generate a DEM in a landscape with a large degree of topographical variation in Marlborough, New Zealand. The GNSS data were used in various interpolation techniques including NN, Topo to Raster and IDW techniques. The quantitative research showed that the Topo to Raster technique showed the most accurate DEM results, while the IDW showed the least accurate results.

Chaplot *et al.* (2006) investigated the suitability of various interpolation techniques across a mountainous region in Laos and undulating landscapes in France. The recommendations following the results of the study indicated that the accuracy of the various interpolation techniques needs to be tested in terms of their applicability to multiple resolution data (Chaplot *et al.*, 2006). Many studies have been focused on modelling and identifying the spatial distribution of errors associated with DEM's in order to remove DEM errors (Aguilar *et al.*, 2010; Hu *et al.*, 2009; Stal *et al.*, 2012).

The above studies show that the accuracy of interpolated elevation is affected by the topography of the area of interest and the interpolation techniques used to create the continuous surface. assessment,

with different interpolation techniques being more and less effective in varying landscapes. In South Africa, the Chief Directorate for National Geospatial Institute (NGI) produces a 5 m resolution elevation dataset that can be used by the public for different purposes. There is a significant gap in assessing the accuracy of the various interpolation outputs based on the NGI dataset against survey-grade elevation data sources. The limitations associated with the application of the 5 m resolution NGI dataset needs to be understood in terms of the identification of spatial distribution errors and the circumstances that lead to these errors. This study therefore aims to compare various interpolation techniques to derive a DEM data for the eventual development of flood-lines using the 5 m NGI elevation contours in the Roodepoort region in Johannesburg, South Africa. The specific objectives of the study are to (1) compare various interpolation techniques conducted on the NGI elevation data source which includes the IDW, NN, Kriging, Spline and Topo to Raster techniques and (2) identify limitations associated with the interpolation accuracy of the NGI dataset. The performances of the interpolators will be evaluated using a high-resolution Light Detection and Ranging (LiDAR) derived DEM. It is expected that the comparisons of the various interpolators will contribute to hydrological modelling in South Africa by listing recommendations and limitations of the application of specific interpolation techniques to the 5 m NGI data source for DEM outputs.

2 METHODS

2.1 Study Area

The study area focuses on a 5-kilometre length of a river that is a tributary of the Wilgespruit River, between Willowbrook and Strubens Valley in Roodepoort, Johannesburg (Figure 1). The channel width ranges from between 5 and 20 m over the length of the study area and flows seasonally between October and March (Climate-data.org, 2019). The study area is composed of an urban residential composition, which is amongst the highest affected land-use classes affected by the effects of flooding (Davis-Reddy *et al.*, 2017).

The Roodepoort region receives approximately 610 mm of rain per year, with the majority occurring during the summer months from November to February (Climate-data.org, 2019). The region is classified as warm and temperate according to the Köppen and Geiger climate classification (Conradie,

2012). The warmest months by average temperature are between November and February.



Figure 1: Research Area - Tributary of the Wilgespruit River, displayed in true colour Red-Green-Blue (RGB) band combination.

2.2 Data

2.2.1 5 m Chief Directorate National Geospatial Contours

The 5 m-resolution contour dataset from the DRDLR is generated by the Intergraph Dual Mass Camera (DMC) which captures stereo imagery at a GSD of 0.5 m (NGI, 2018). The NGI also contracts service providers with similar cameras to acquire data owing to the scale of the operation. Currently, the NGI aims to capture 40% of the country every 3 years and the remaining areas every 5 years. The dataset included in this research is the 5 m contour dataset (referred to as the NGI dataset), which was last updated 8 December 2009, for the study area.

The 5 m resolution contour dataset has the largest spatial coverage compared with more recent high-resolution survey campaigns that have been commissioned by the City of Johannesburg (COJ) Municipality. While higher resolution (that is, to smaller GSD) datasets are available for metropolitan areas in South Africa, sites that fall outside of the metropolitan area demarcations are at best covered by the 5 m contour offering. As such, the 5 m NGI dataset is a popular choice among specialists who seek to apply topographical elements to their respective studies.

2.2.2 Light Detection and Ranging Point Cloud

The LiDAR data for the study area was obtained from the COJ Municipality Corporate Geo-informatics Department. LiDAR is a popular method of surveying

that uses an active remote sensing system composed of at least three sensors, the Inertial Measurement Unit (IMU), the Global Positioning System (GPS) and the laser scanner (Csanyi & Toth, 2007). A target is illuminated by a light source through a laser beam and the time taken for the reflected beam to return to the sensor allows for the calculation of survey-grade measurements relating to the linear position of the target from the sensor (Vosselman, 2003). Advancements in optical and computing technologies have seen the emergence of LiDAR as a rapid and accurate terrain mapping tool (Lohani & Ghosh, 2017). The COJ municipality region distributes an aerial-based LiDAR data that is acquired by a contracted service provider every three years. The data sourced for this study was acquired in June 2012.

The native format for the LiDAR data includes American Standard Code for Information Interchange (ASCII)-based text files that contain information relating to each point's location and elevation, which collectively form a point cloud. The LiDAR point clouds used in the present study had a point density of 0.2 points per square meter with an approximate average spacing between neighbouring points of 2 m. Therefore, LiDAR is acknowledged for its survey-grade level of accuracy (Vosselman, 2003; Lohani & Ghosh, 2017). The horizontal accuracy of the LiDAR data had a 0.048 m root mean square error (RMSE), and a vertical accuracy of 0.32 m RMSE as verified using a network of seven ground control points. The points were classified into ground and non-ground points by the data supplier, with the ground points representing the physical ground level, while the non-ground points represented all features above ground including vegetation and structures. The ground points were used in the present study to serve as the baseline dataset to evaluate the relative accuracy of the different interpolation techniques applied to the 5 m elevation contour dataset.

2.3 Analysis

To produce continuous digital representations of a surface, interpolation techniques were derived to calculate unknown values that lie between known values. In this study, five interpolation techniques conducted on the 5 m resolution NGI dataset were compared, namely IDW, NN, kriging, spline, and Topo to Raster algorithms.

IDW is a non-linear, deterministic interpolation technique that computes a weighted average of a value from sample points in close vicinity to determine the value of non-sampled points (Robinson & Metternicht, 2003). The IDW principle was first

presented by Shepard (1968) for improved efficiency of the central processing unit time. Today, the IDW process is one of the most widely applied methods of interpolation in the hydrological environment. The IDW principle assumes that values which are close together are more alike than values that are further away. To calculate the value of an unknown point at a location, the weighted average of the surrounding known values is calculated and assigned to the unknown point. Known values that are closer to the location of the unknown point are given a higher weighting ranking in the calculation, and therefore have a larger influence on the determination of the unknown value, opposed to known values that are further away. Definitions of the neighbouring radius for the calculation and the power function representing the inverse distance relationship between the points are critical parameters for this interpolation method. The formula for the IDW interpolation is defined as $Z_0 = \frac{\sum_{i=1}^N z_i d_i^{-n}}{\sum_{i=1}^N d_i^{-n}}$, where Z_0 = value of variable Z in point I; Z_i = the sample in point I; d_i = distance to the sampled point from the unknown point; N = coefficient that defines the weight that will be based on the inverted distance function; n = total number of predictions allowed for each validation (Shepard, 1968).

The NN Interpolation model is based on the Sibson interpolation model, where values are assigned to un-sampled points based on the construction of Thiessen polygons which work together to form areas of overlap (Sibson, 1980). The polygons are formed across all known values surrounding the unknown value by connecting all common values into a network of Thiessen polygons which represent all known values. A new Thiessen polygon is then generated over the unknown value, and the proportion of the overlap between this new polygon versus the network of intersecting polygons previously generated define the weighting system to be used. The formula used for the NN interpolation is identical to IDW, with the only difference coming from the method used to calculate the weightings. The NN interpolation formula is defined as $\hat{Z}(u) = \frac{\sum_{i=1}^N \lambda_i(u) \times z_i}{\text{Total area of polygon}}$, where $\lambda_i(u) = \frac{\text{area contributed by Polygon } i}{\text{Total area of polygon}}$ and $u = (x,y)$ location of query point (Rukundo & Cao, 2012).

Kriging is a stochastic local interpolation technique that computes the value of non-sampled points in a similar way to IDW, with the exception that there is more control on the weighting system that determines unknown values based on distance (Robinson & Metternicht, 2003). The kriging model

was developed by Danie Krige, who formed the basis of what would later be called the kriging process in 1951 through research presented in the Journal of the Chemical, Metallurgical and Mining Society of South Africa in the 1960s (Cellmer, 2014). Krige (1951) applied the kriging technique to survey two gold mines to understand resource estimation based on borehole data. An ordinary kriging equation is defined as $Z(s_0) = \sum_{i=1}^n \lambda z(s_i)$, where, λ = weights assigned to each known value, where all weights sum to a unity which enables unbiased estimations which are defined as $\sum_{i=1}^n \lambda_i = 1$. The matrix equation calculating the weights is defined as $C = A^{-1} \times b$, where A = matrix of semi-variance between the known values; b = estimated semi-variances between the known values and unknown value, represented by a vector (Krige, 1951; Krige, 1952).

The spline interpolation is a piecewise polynomial interpolation method that creates a smooth raster surface from the known sample points using a 2-D minimum curve technique (Robinson & Metternicht, 2003). The resulting surface passes through all known sample points. The spline method is mathematical in nature and takes the form of a cubic equation whereby each known data point has a cubic equation through which all splines pass (Robinson & Metternicht, 2003). Jenkins (1927) and Schoenberg (1946) can be credited with the origins of the spline method of interpolation. The spline cubic equation is defined as $S(x, y) = T(x, y) + \sum_{j=1}^n \lambda_j R(r_j)$, where $j = 1, 2, \dots, N$, N is the number of points, λ_j are the coefficients found by the linear equation solution and r_j is the distance from the point (x,y) to the j^{th} point (Meijering, 2002).

ANUDEM is based on a program developed to interpolate elevation values across a topographical surface by Hutchinson (1988). The algorithm generates elevation models that are hydrologically conducive to network extraction (Callow *et al.*, 2007). In the 1980s, a study done by Mark (1984) proposed an algorithm for automatically delineating a drainage network from DEM data. This study gave rise to the need for hydrological correction algorithms in the DEM interpolation process which includes the development of the ANUDEM. This interpolation technique provides a compromise between local interpolation methods such as IDW and global interpolation methods such as kriging, by allowing the resultant DEM values to follow abrupt changes in terrain which include streams, ridges and cliffs, thus preserving topographical continuity (Pavlova, 2017). The Topo to Raster interpolation is the only algorithm featured in ArcGIS that is preferentially applied to

contour datasets. The Topo to Raster interpolation is defined by the equation $J_1(f) = \int (f_x^2 + f_y^2) dx dy$, where J_1 is known as a local interpolation technique that is well-suited for features with a better resolution. Then $J_2(f) = \int (f_{xx}^2 + f_{xy}^2 + f_{yy}^2) dx dy$, where J_2 is known to create unrealistically flat surfaces as commonly seen by global interpolation techniques. Hutchinson's ANUDEM program revolves around a compromise between J_1 and J_2 as follows: $J(f) = 0.5 \times h^{-2} J_1(f) + J_2(f)$, where h is the spatial resolution of the output surface model (Hutchinson, 1988).

2.4 Accuracy Assessment

A buffer measuring 100 m was created around the river's centreline. Points were then generated at 100 m intervals along the extent of the buffer, from which LiDAR elevations were extracted within a 5 m average distance from each point, resulting in a total of 103 LiDAR spot elevations. Figure 2 shows the positions of the spot elevation points, plotted against a 2018 WorldView-2 derived satellite image that is rendered in red, green and blue (RGB). These elevation values, along with their X and Y positions, represent the most accurate remotely sensed dataset available for this study and were therefore used as reference data to compare the different surfaces created using the five interpolators applied to the 5 m contour data. While a field-collected differential real-time kinematic GPS system will provide the highest level of accuracy, the intention of the research presented is to utilise practical and readily available datasets, such as the COJ distributed LiDAR. Elevation values of the five interpolated surfaces were extracted at each of the above-mentioned LiDAR spot elevation locations. The T-test and residual analysis was used to compare the interpolated surfaces against the baseline LiDAR elevation values.

2.4.1 Comparing the Output Elevations of the Interpolated DEMs against the Reference LiDAR Elevations

The T-test is a statistical procedure that is commonly used when investigating the relationship between variables by comparing the means on the dependent variables against the baseline or independent variable (Green & Salkind, 2012). The T-test was chosen due to the flood extent comparisons involved at each measurement station, where more than one dependent set of results is compared to the baseline LiDAR flood-line extents. The P-value from the T-test output

is used to assess the degree of difference between the means of the interpolation elevation versus the baseline LiDAR elevation. The applied T-test formula is a generalisation of a two-sample T-test (Ostertagova & Ostertag, 2013) and is defined as $F = \frac{\text{Mean square between groups (MSG)}}{\text{Residual Mean Square (RMS)}}$ where $MSG = \frac{\sum_{i=1}^k \left(\frac{T_i^2}{n_i} \right) - G^2/n}{k-1}$ and $RMS = \frac{\sum_{i=1}^k \sum_{j=1}^{n_i} Y_{ij}^2 - \sum_{i=1}^k \left(\frac{T_i^2}{n_i} \right)}{n-k}$, where Y_{ij} is the observation distances from the stream centreline for each output, T_i is the sum of each group of distances from the stream centreline, G is the total of all observations being compared for the variance (model output being assessed versus baseline LiDAR output), n_i is the number of observations in group i and n is the total number of observations being analysed for the variance. The T-test and associated P-values were calculated using Microsoft Excel (Microsoft Corporation, 2019).

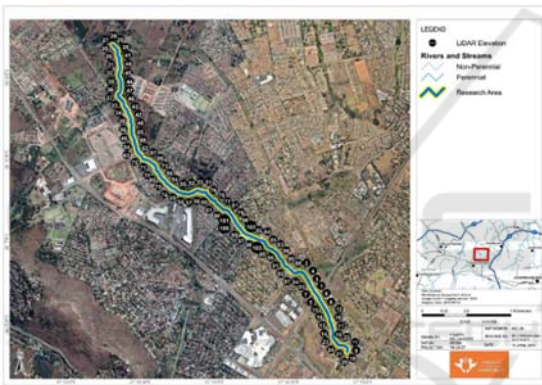


Figure 2: Location of observations for analysis, displayed in true colour RGB band combination.

2.4.2 Identification of Outliers from the Interpolated DEMs against the LiDAR Reference Data

Analysis of residuals forms part of a regression analysis which is designed to assess model adequacy (Martin *et al.*, 2017). Regressions are typically applied to assess the accuracy of a predicted model against actual values (Martin *et al.*, 2017). Because the research purpose is accuracy assessment, as opposed to model fitting, regression analysis was not chosen as an accuracy assessment tool in this research. However, components of the regression analysis remain useful tools in location-based analytics, such as the residual analysis which allows for reference to a specific observation and its associated spatial location. Residuals are defined as the vertical distance (r_i) between the observed

measurement and the predicted measurement ($r_i = y_i - \hat{y}$), represented by a linear regression line. In this research, the observed distance (y_i) represents the linear regression from the baseline LiDAR elevation while the predicted measurement (\hat{y}) represents the vertical elevation difference between the interpolation surface being assessed (Topo to Raster, kriging, NN, IDW, spline).

Outlier identifications in data have been applied successfully through the usage of standardised residuals (Sousa *et al.*, 2012; Miller, 1993, Salekin *et al.*, 2018) and are defined by the formula $r_s = \frac{r_i}{s}$, where the standardised residual (r_s) is the residual value (r_i) divided by its standard deviation (s). At a 95% confidence level, it is expected that 95% of the data falls within 2 standard deviations of the mean (Sousa *et al.*, 2012). Data points falling lower than -2 and higher than 2 on the standardised residual plot will therefore represent outliers. The incorporation of a standardised residual analysis allows for the identification of interpolated elevation output observations that are significantly different to the baseline LiDAR elevation values, which in turn allows for a spatial expression of the results observed.

The methodology starts with the running of the various interpolation procedures. As the focus of the assessment is on the influence of interpolation techniques on hydrological modelling environments, a streamflow analysis was run on the baseline LiDAR dataset, from which a 100 m buffer was generated. LiDAR points were then selected using proximity analyses at every 100 m interval along the extent of the buffer. Interpolated elevation values were then extracted from each interpolation process at each LiDAR elevation point every 100 m along the buffer zone. All GIS-based processing procedures were conducted using ArcGIS (ESRI, 2019). The interpolated elevation observations were then compared against the LiDAR elevations using a T-test and residual analysis in Microsoft Excel (Microsoft Corporation, 2019).

A buffer measuring 100 m was created around the river's centreline. Points were then generated at 100 m intervals along the extent of the buffer, from which LiDAR elevations were extracted within a 5 m average distance from each point, resulting in a total of 103 LiDAR spot elevations. These elevation values, along with their X and Y positions, represent the most accurate remotely sensed dataset available for this study and were therefore used as reference data to compare the different surfaces created using the five interpolators applied to the 5 m contour data. While a field-collected differential real-time kinematic GPS system will provide the highest level

of accuracy, the intention of the research presented is to utilise practical and readily available datasets, such as the COJ distributed LiDAR. Elevation values of the five interpolated surfaces were extracted at each of the above-mentioned LiDAR spot elevation locations. The T-test and residual analysis was used to compare the interpolated surfaces against the baseline LiDAR elevation values.

3 RESULTS

3.1 Differences between Interpolated Elevations and LiDAR Elevations

The T-test presented in this section yields information on the degree of variance between the elevation values obtained from each interpolation against the baseline LiDAR elevation values. The T-test was run at an alpha = 5%. The outputs from the T-test for the various interpolation algorithms are presented in Table 1 which has been sorted from most accurate to least accurate.

The Topo To Raster interpolation had the highest correlation with the baseline LiDAR elevation with a P value of 0.75. The lowest P value obtained indicates a relatively strong correlation to the LiDAR baseline elevations when compared against the other interpolation techniques. The mean value from the Topo to Raster techniques elevation values are close to the mean value of the LiDAR elevations (1553.99), with the Topo To Raster interpolation generally underestimating the elevation by 1.10 m.

The T-test results indicate NN to have the second highest correlation to the baseline LiDAR elevation with P value of 0.78. The P value indicates a relatively good correlation to the LiDAR baseline elevations when compared against the other interpolation techniques. The mean value from the NN techniques elevation values are close to the mean value of the LiDAR elevations (1553.99), with the NN interpolation generally underestimating the elevation by 0.96 m. The Kriging T-test results show this technique to marginally be the third most accurate interpolator with results similar to the NN technique with a P value of 0.79. The IDW T-test results are within close range of the Kriging and NN interpolators, showing a relatively good correlation to the baseline LiDAR elevations with P value of 0.79. Both Kriging and IDW mean outputs indicate a general underestimation of the elevation by 0.95 m and 0.93 m respectively in relation to the LiDAR mean value.

The spline T-test results show the highest variance to the baseline LiDAR by far with a P value of 0.00. The negligible P value and highest mean deviation from the LiDAR elevation with a general overestimation of -69.84 m indicate that the spline interpolation technique is unsuitable for deriving a suitable DEM from the NGI 5 m dataset.

Table 1: T-test results across all interpolation techniques results. Each interpolation was compared against the LiDAR mean elevation of 1553.9 m.

Interpolation Technique	Mean Elevation (Meters above mean sea level)	Mean Difference between LiDAR and Interpolator (meter)	*P Value
Topo To Raster (ANUDEM)	1553.06	0.93	0.754
NN	1553.04	0.95	0.787
Kriging	1553.04	0.95	0.787
IDW	1552.89	1.10	0.791
Spline	1623.83	-69.84	0.000

*P value was measured using 95% confidence level

3.2 Identification of Outliers from the Interpolated DEMs Relative to the LiDAR Data

The plotted residual results are presented for each interpolation technique in Figure 3. The results graphically illustrate the outliers of significance that can be related to a spatial location, which forms a platform for the subsequent discussion around the results seen. Residuals of Topo to Raster, NN, IDW and kriging share a similar distribution throughout the plot. The spline residual plot results resemble the same general distribution as the other interpolators but appear to have larger variances along the residual plot.

The Topo to Raster, NN, kriging and IDW residual points all show a dependent positive correlation to the LiDAR elevations with a wave-form trend about the Y-axis. Elevations of 1500–1540 m and 1560–1600 m show a general underestimation of elevation values by the Topo to Raster interpolation. For elevation values of 1540–1560 m, the Topo to Raster interpolation overestimates the elevations. Highly significant outliers occur at higher elevation values at around 1600 m. The IDW and kriging interpolation outputs have similar

standardised residual plots, while the Topo to Raster and NN interpolation outputs share similarities in their standardised residual plots. The spline interpolation residual points also show a general dependent positive correlation to the LiDAR elevations, but in comparison to the other interpolators, the spline results have a larger residual variance. Larger underestimations in elevation values are seen at 1530–1550 m, with the same general observation of higher overestimations of elevations at 1600 m.

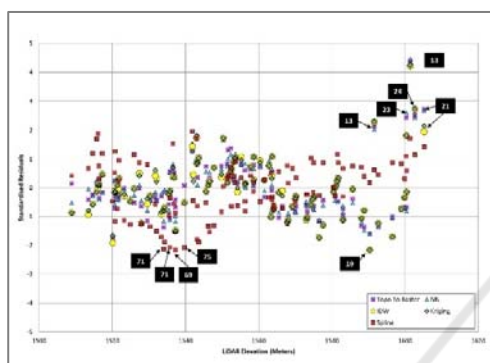


Figure 3: Combined standardised residuals across all interpolation techniques with significant outliers identified with labels.

Table 2 shows the name and location of the elevation values that were identified through the residual plot shown in Figure 3. Observations 13, 14, 21, 23 and 24 show overestimations of the elevation across all interpolation techniques except for the spline technique. Observation 19 shows underestimations of elevation in the kriging and IDW technique while observations 69, 70, 71 and 75 show underestimations of the elevation only in the spline technique.

Table 2: Significant outliers Identified from standardised residual plot analysis.

Topo To Raster		NN		Kriging		IDW		Spline
Standardised Residual	Distance to LiDAR Elevation	Standardised Residual						
2.14	-5.20	2.02	4.91	2.30	-5.74	2.29	5.75	0.62
4.39	10.63	4.46	10.83	4.24	10.60	4.22	10.60	1.71
-1.61	-3.90	-1.61	-3.90	-2.16	-5.41	-2.17	-5.44	0.17
2.73	6.62	2.67	6.49	2.15	5.37	1.95	4.89	1.42
2.45	5.93	2.62	6.35	1.82	4.56	1.81	4.55	1.10
2.52	6.12	2.44	5.91	2.74	6.86	2.79	6.85	1.14
-0.69	-1.67	-1.18	-2.86	-1.51	-3.77	-1.49	-3.74	-2.17
-1.06	-2.57	-1.13	-2.74	-0.13	-0.32	-0.12	-0.29	-2.07
-1.38	-3.34	-1.17	-2.84	-0.80	-2.00	-0.78	-1.97	-2.14
0.07	0.17	-0.51	-1.24	-0.54	-1.34	-0.52	-1.31	-2.09

Figure 4 shows the identified locations of the significant residual outliers in the upper section of the tributary (Locations 11, 13, 14, 19, 21, 23 and 24). The downstream section of the tributary shows a higher correlation between the LiDAR elevation and

interpolated algorithms that are within a 95% confidence level of vertical elevation difference. A large concentration of outliers can be seen in the upstream section of the tributary, where 5 of the 6 observation outliers identified are overestimations of elevation. The remainder of residual outliers identified (69, 70, 71 and 75) are all identified from the spline interpolation with significant elevation deviations (all 13 m under the LiDAR elevation).



Figure 4: Identified standardised residual outlier locations, displayed in true colour RGB band combination.

4 DISCUSSION

The results obtained in the interpolation output compared against the reference LiDAR data indicate that the Topo to Raster interpolation technique yields marginally more accurate DEM surfaces than the other interpolators, based on the T-test. The Topo to Raster results agree with existing bodies of research (Arun, 2013; Salekin *et al.*, 2018) indicating that the Topo to Raster technique preserves critical components of the hydrological environment and by doing so, is the most accurate under these conditions. The spline interpolation technique was the most inaccurate and is unsuitable for the application on the 5 m NGI dataset to create a DEM. These results from the spline methodology are inconsistent with findings from Erdogan (2009) and Pavlova (2017) who found that the spline methodology yielded marginally more accurate results in comparison to other interpolations assessed. It must, however, be noted that Erdogan (2009) utilised a thin-plate spline algorithm which is a derivative of the original spline technique; this was not used in the research presented here, and Pavlova's (2017) findings are representative of an area with low topographical variations. All other interpolation techniques assessed in the results presented as part of this research show good applicability with marginal differences in variation to the baseline LiDAR.

Spatial representations of the outliers as identified from the residual analysis reveal a large concentration of points to the upper part of the tributary which fall on a garden refuse site (Figure 4). Due to the differences in the temporal acquisition of the data, the garden refuse site would have undergone topographical changes to its the baseline LiDAR (acquired in June 2012) compared to NGI (acquired in December 2009). Figure 5 illustrates the progression of the area, identified as the Weltevreden Park PickitUp garden refusal site, between 2006 and 2019 which shows the visible changes in topography over 13 years. Changes in the surface topography across this site over time have a direct influence on the elevation values observed during the LiDAR and NGI data acquisitions. These elevation value differences are prominent in the residual analysis, which shows a large concentration of residuals with a variance larger than 5 m in and around the refuse site. The residual interpretation further indicates the spline interpolation’s output is unsuitable for accurate DEM interpolation from the 5 m NGI data source.



Figure 5: PickitUp garden refuse site surface changes: 2006-2019, displayed in true colour RGB band combination.

The differences in elevation values between the NGI versus the LiDAR data reveals large differences in elevation values in the refuse site region, located in the upper section of the tributary (Figure 2.7). The NGI surface along this section is almost constantly below the LiDAR surface which shows clear definitions of a dump feature (Figure 2.8). This is indicative of changes in the surface between the acquisition of the 5 m NGI dataset (December 2009) and the LiDAR dataset (June 2012) which is statistically shown with the underestimation of the elevation values with the 5 m NGI dataset. The profile comparisons show a high degree of variance with regards to topographic changes that have occurred over the dumpsite, highlighting differences in temporal resolution as shown in Figure 6.

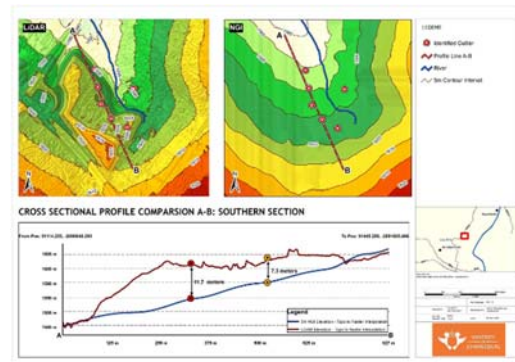


Figure 6: Profile comparisons for LiDAR (Left) versus NGI (Right) along A-B.

5 CONCLUSION

The findings of this study indicate that the Topo to Raster interpolation technique is the most favourable for the 5 m contour data of the localised study area. The results also indicate that while the application of the Topo to Raster technique yielded the most accurate results, the NN, kriging and IDW techniques were close to the Topo to Raster technique. These results imply that the application of the NN, kriging and IDW interpolation techniques to the 5 m NGI dataset will yield DEMs with similar vertical accuracy.

While the results indicate that the Topo to Raster technique is the most accurate, it must be acknowledged that certain interpolation techniques are likely to yield the most favourable results in the environments for which they were originally developed. The Topo to Raster interpolation algorithm was specifically formulated for its application in hydrological environments (Hutchinson, 1988), while the geostatistical method evaluated in this research (kriging) and local methods (NN and IDW) are limited by the resolution and spread of data (Al Mashagbah *et al.*, 2012). Research into the interpolation technique to be applied and its favourability to different spatial distributions of data should always be taken into account when interpolating elevation datasets (Cellmer, 2014). Due to advancements in technology and information, it is also likely that the defining geometry (point, line or polygon) of the elevation data sources may change from line-based contour elevations to point-cloud elevation formats, which will also play a significant role in determining the ideal interpolation technique to apply.

The results presented in this research are specific to the application on the freely and nationally

distributed South African NGI contour dataset. The residual analysis indicated substantial differences in elevation between areas for the reference LiDAR and NGI datasets, which is attributed to differences in temporal resolution. As access to spatial information in South Africa increases in association with advancements in survey techniques, future assessments should be performed on the most temporally relevant data available. The findings indicate that while the usage of lower spatial resolution datasets such as the 5 m data used in the present study may be acceptable in terms of RMSE, the need for access to more temporally relevant datasets is crucial to accurately represent topographical information for an area.

REFERENCES

- Aguilar, F.J., F. Aguera, M.A. Aguilar. & F. Carvajal. (2005). Effects of terrain morphology, sampling density, and interpolation methods on grid DEM accuracy. *Photogrammetric Engineering and Remote Sensing*, 71: 805–816.
- al Mashagbah, A., R. Al-Adamat. & E. Salameh. (2012). The use of Kriging Techniques within GIS Environment to Investigate Groundwater Quality in the Amman-Zarqa Basin/Jordan. *Research Journal of Environmental and Earth Sciences*, 4: 177-185.
- Arun, P. V. (2013). A comparative analysis of different DEM interpolation methods. *The Egyptian Journal of Remote Sensing and Space Sciences*, 16(2): 133-139.
- Academy of Science of South Africa (ASSAf), (2020). *Quest: Science for South Africa*, 16(2).
- Callow, J, N., G.S Boggs. & K. P van Niel. (2007). How does modifying a DEM to reflect known hydrology affect subsequent terrain analysis? *Journal of hydrology*, 332(1-2): 30-39.
- Cellmer, R. (2014). The possibilities and limitations of geostatistical methods in real estate market analyses. *Real Estate and Valuation*, 22(3): 54-62.
- Chaplot, V., F. Darboux, H. Bourenane, S. Leguedois, N. Silvera. & K. Phachomphon. (2006). Accuracy of Interpolation Techniques for the Derivation of Digital Elevation Models in Relation to Landform Types and Data Density. *Geomorphology*, 77: 126-141.
- Climate-data.org. (2019). Roodepoort Climate. Available from <https://en.climate-data.org/africa/south-africa/gauteng/roodepoort-232/>.
- Conradie, D. C. U. (2012). South Africa's Climatic Zones: Today, Tomorrow. International Green Building Conference and Exhibition, Future Trends and Issues Impacting on the Built Environment, Sandton, July 25-26.
- Council for Scientific and Industrial Research (CSIR). (1999). Ecologically Sound Urban Development. Available from https://www.csir.co.za/sites/default/files/Documents/Chapter_05_08_02_-_Vol_I.pdf.
- Csanyi, N. & C.K. Toth. (2007). Point positioning accuracy of airborne lidar systems: A rigorous analysis. *International Archives of Photogrammetry, Remote Sensing and Spatial Information Systems*, 36(1):107-111.
- Davis-Reddy, C.L. & K.Vincent. (2017). *Climate risk and vulnerability: A handbook for Southern Africa* (2nd Edition), CSIR, Pretoria, South Africa.
- Department of Water and Sanitation (DWS). 2017. The quaternary drainage regions. Available from <http://www.dwa.gov.za/iwqs/wms/data/000key2data.asp>.
- Erdogan, S. (2009). A comparison of interpolation methods for producing digital elevation models at the field scale. *Earth Surface Processes and Landforms*, 34: 366-376.
- ESRI 2019. ArcGIS Desktop: Release 10.7. Redlands, CA: Environmental Systems Research Institute.
- Green, S.B. & N.J. Salkind. (2010). *Using SPSS for Windows and Macintosh: Analysing and understanding data* (5th Edition). Upper Saddle River, New Jersey: Pearson Education Incorporated.
- Hutchinson, M.F. (1988). Calculation of hydrologically sound digital elevation models, Third International Symposium on Spatial Data Handling at Sydney, Australia, vol. 3, no. 1, pp.120–127.
- Jenkins, W.A. (1927). Graduation based on a modification of osculatory interpolation. *Trans. Actuar. Soc. Amer*, 28:198-215.
- Johnson, M. R., C.R. Anhaeusser. & R.J. Thomas. (2006). *The Geology of South Africa*. Council for Geoscience.
- Krige, D.G. (1951). A statistical approach to some basic mine valuation problem on the Witwatersrand. *Journal of the Chemical, Metallurgical and Mining Society of South Africa*. 12: 119–139.
- Krige, D.G. (1952). A statistical analysis of some of the borehole values in the Orange Free State goldfield. *Journal of the Chemical, Metallurgical and Mining Society of South Africa*, 9: 47–64.
- Lohani, B. & S. Ghosh. (2017). Airborne LiDAR technology: A review of data collection and processing systems. *Proceedings of the National Academy of Sciences, India Section A: Physical Sciences*, 87(1):567-579.
- Manuel, P. (2004). Influence of DEM interpolation methods in drainage analysis. *GIS in Water Resources*, 8: 32-28.
- Mark, D.M. (1984). Automatic detection of drainage networks from digital elevation models. *Cartographica*, 21(2-3): 168-178.
- Martin, J., A. David. & A. Garcia Asuero. (2017). *Fitting Models to Data: Residual Analysis, a Primer*. *Intech*. Available from: <http://dx.doi.org/10.5772/68049>.
- Matheron, G. (1963). Principles of geostatistics. *Economic Geology*, 58: 1246-1266.
- Meijering, E. (2002). A chronology of interpolation: From ancient astronomy to modern signal and image processing. *Proceedings of the IEEE*, 90(3): 319-342.

- Merz, R. & G. Blöschl. (2008). Flood frequency hydrology: Temporal, spatial, and causal expansion of information. *Water Resources Research*, 3:13-20.
- Microsoft Corporation, 2019. Microsoft Excel (Windows 10 version), Available at: <https://office.microsoft.com/excel>.
- Miller, J.N. (1993). Outliers in experimental data and their treatment. *Analyst*, 118(5):455-461.
- Nkwunonwo, U.C., M. Whitworth. & B. Baily. (2020). A review of the current flood modelling for urban flood risk management in the developing countries. *Scientific African*. 7: e00269.
- Ostertagova, E. & O. Ostertag. (2013). Methodology and application of one-way ANOVA. *American Journal of Mechanical Engineering*, 1(7):256-261.
- Pavlova, A.I. (2017). Analysis of elevation interpolation methods for creating digital elevation models. *Optoelectron. Instrument. Proc*, 53(2): 171–177.
- Robinson, T. B. & G. Metternicht. (2003). A comparison of inverse distance weighting and ordinary kriging for characterizing within-paddock spatial variability of soil properties in Western Australia. *Cartography*, 32(1): 11-24.
- Rukundo, O. & H. Cao. (2012). Nearest Neighbor Value Interpolation. *International Journal of Advanced Computer Science and Applications*, 3: 25-30.
- Saksena, S. & V. Merwade. (2015). Incorporating the effect of DEM resolution and accuracy for improved flood inundation mapping. *Journal of Hydrology*, 530(1):80-194.
- Salekin, S., J.H. Burgess., J. Morgenroth., E.G. Mason., D.F. Meason. (2018). A comparative study of three non-geostatistical methods for optimising digital elevation model interpolation. *ISPRS International Journal of Geoinformatics*, 7: 300-308.
- Shepard, D. (1968). A two-dimensional interpolation for irregularly-spaced data. 23rd ACM National Conference, Brandon Systems Press, Princeton, New Jersey, pp. 517–524.
- Sibson, R. (1980). *Interpolating Multivariate Data: A Brief Description of Natural Neighbour Interpolation*. New York: Wiley.
- Smithers, J. C. (2012). Methods for design flood estimation in South Africa, *Water SA*, 38(4): 633–646.
- Sousa, J.A., A.M. Reynolds. & A.S. Ribeiro. (2012). A comparison in the evaluation of measurement uncertainty in analytical chemistry testing between the use of quality control data and a regression analysis. *Accredited Quality Assurance*, 17(1):207-214.
- South Africa. Department of Rural Development and Land Reform, Chief Directorate: National Geo-spatial Information (NGI). (2018). Chief Directorate for Surveys and Mapping. Available from: <http://www.cdsm.gov.za>.
- South Africa. Department of Rural Development and Land Reform, Chief Directorate: National Geo-spatial Information (NGI). (2014). National Landcover Classification – Geo Terra Image. Available from <http://www.geoterraimage.com/uploads/GTI%202013-14%20SA%20LANDCOVER%20REPORT%20-%20CONTENTS%20vs%2005%20DEA%20OPEN%20ACCESS%20vs2b.pdf>.
- Stal, C., A. De Wulf., P. De Maeyer., R. Goosens., T. Nuttens., F. Tack. (2012). Statistical comparison of urban 3D models from photo modelling and airborne laser scanning. *International Multidisciplinary Scientific GeoConference-SGEM*, 12: 901-908.
- Teng, J., A.J. Jakeman, J. Vaze, S. Kim, B. Croke. & D. Dutta. (2017). Flood inundation modelling: A review of methods, recent advances and uncertainty analysis. *Environmental Modelling and Software*, 90: 201-216.
- Vosselman, G. (2003). 3D reconstruction of roads and trees for city modelling. *The International Archives of the Photogrammetry, Remote Sensing and Spatial Information Sciences*, 34(1): 211-216.
- Zimmerman, D., C. Pavlik, A. Ruggles. & M. Armstrong. (1999). An experimental comparison of ordinary and universal kriging and inverse distance weighting. *Mathematical Geology*, 31: 475-390.